A SEMI-ANALYTICAL MODEL FOR NON-MACH PEAK PRESSURE OF UNDERWATER ACOUSTIC PULSES FROM OFFSHORE PILE DRIVING

Marshall V. Hall
Moya Crescent, Kingsgrove NSW 2208, Australia
marshallhall@optushome.com.au

The equations of motion for the axial and radial displacements in a hammered semi-infinite pile comprise a system of coupled partial differential equations which are solved by taking their Fourier Transforms. The impact generates a pulse of axial and radial vibrations (a bulge) that disperses slightly as it travels down the pile. The damping rate is high at frequencies close to the radial resonance frequencies of the pile. After the bulge arrives at a given depth, the axial displacement increases with time to an asymptote, whereas the radial displacement rapidly rises to a peak and then decays to zero. Although the bulge constitutes a moving sound source, the radiated peak pressure is computed as if it were stationary at a number of depths. The ratio of pressure to fluid particle velocity at the pile wall is obtained by assuming the pile to be in a homogeneous medium. The spectrum of radial displacement, which is subject to radiation loading, is expressed as a closed-form algorithm in terms of the hammer impact velocity, the radius and wall thickness of the pile, and the Poisson ratio, longitudinal sound-speed, and density of the pile material. The radial displacement algorithm is linked to two simple models for sound radiation from a cylinder: near-field from depth-independent vibration, and far-field from depth-dependent vibration. These models are applied to a published case for which radiated peak pressures were measured and computed at a fixed range from a steel pile, using a Finite Element Model. The near-field/ depth-independent model overestimates the peak pressure, since it assumes that the cylinder is of infinite length. The far-field/ depth-dependent model underestimates the observed peak pressure. If a sound source moves supersonically perpendicular to a sound propagation path then coherent multipaths arrive quasi-simultaneously (Mach waves). The first model over-estimates the Mach wave pressure from a finite cylinder, while the second model neglects Mach waves altogether. A non-rigorous method for estimating the Mach wave pressure is described.

INTRODUCTION

Offshore pile driving radiates regular pulses of loud noise underwater, and a substantial amount of data has been presented in the literature on the measured peak pressure of these pulses. The peak pressure at a horizontal range of 10 m can be in the region of 1 atmosphere (100 kPa). Pile driving pulses are "brief, broadband, atonal" and "characterised by a relatively rapid rise from ambient pressure to a maximal pressure value followed by a decay period that may include a period of diminishing, oscillating maximal and minimal pressures" [1]. The frequency of successive pile driving pulses (the blow rate) is usually between 15 and 30 per minute [2]. The individual pulse duration can vary between 15 and 90 ms, and is most likely to lie between 25 and 40 ms [3].

Although the quantity of descriptive data on underwater noise from offshore pile driving is large, there have been few papers that attempt to model the physics of the impact and the consequent sound radiation. It is generally accepted that the major underwater signals originate from radial vibration (bulging) of that portion of the pile that is submerged. Since the bulge travels downward faster than sound travels through water, the first arrival at a hydrophone will originate at a point on the pile a little shallower than itself, and the trailing signal will be due to multipaths from portions of the pile both above and below the originating point. A significant paper [4] reported the use of a finite-element model of the sound generated by a simple impact hammer. The results were entirely numerical, and their sensitivities to the various input parameters cannot be ascertained by examining the paper. The dominating effect of the simultaneous arrivals of multipaths from the pile (the "Mach wave") was included [4].

There has been significant theoretical work on onshore pile driving, including analytical modelling [5-7]. These and other numerical models were concerned only with axial vibration however, and did not present material that could be significantly applied to radial vibration.

The objective of the present paper is to present a semi-analytical model for the peak pressure of non-Mach radiation, since such a model allows the relative importance of the driving parameters to be estimated. Although the effect of Mach waves is not treated explicitly, the results obtained do suggest a method by which it may be estimated.

ASSUMPTIONS

A pipe pile is modelled as a thin vertical cylindrical shell of an elastic material such as steel. Absorption of sound (conversion to heat) in the material is represented by a small loss factor. The pile is semi-infinite in length. Although other analyses have treated finite lengths and thus include echoes from the pile toe, this aspect is not addressed here. The upper

portion of the pile is in air and finite in length. The remainder is submerged in water of infinite depth. The hammer is a compressible solid vertical cylinder with the same density and Young modulus as the pile. It has a finite mass and therefore length. Reflections from the top of the hammer following impact are however neglected. Since the hammer is compressible, the initial velocity of the pile face is estimated by assuming the interfaces satisfy the principle of momentum conservation.

The hammer strikes the pile instantaneously and uniformly over its face, and does not cause the pile to twist or bend. The ensuing axial and radial displacements will therefore not vary significantly with azimuthal (polar) angle around the pile axis. Only the sound radiated shortly after impact is addressed.

Each of the two external media allows sound waves to radiate from the pile. The effect of the medium on the pile vibration is obtained by assuming the radial velocity of the pile wall generates strain in the external medium, and the consequent stress (pressure) has the same effect on the cylinder as if it were an external pressure applied to a cylinder in-vacuo [8]. The wall vibration is thus subject to feedback.

For a hydrophone at a given horizontal range from the pile and depth beneath the water surface, the problem of determining the pressure waveform from the moment the leading edge of the downward travelling bulge crosses the water surface until it reaches great depth is beyond the scope of the present paper. Instead, it is assumed that the peak pressure occurs a short time (the travel time for the horizontal range) after when the leading edge is at the same depth as the hydrophone. For the purpose of modelling, the bulge is considered to be vibrating at that fixed depth; the vertical motion of the bulge down the pile is neglected. The aperture of the pile that determines the waveform and hence peak pressure is the whole pile beneath the water surface.

The radial displacement algorithm to be produced will be linked to two simple models (near-field and far-field) for sound radiation from a cylinder. Modelling of Mach-wave multipaths that arrive simultaneously due to the supersonic speed of the sound source is included in the near-field model, but neglected in the far-field model.

It is assumed that reflection of underwater sound waves by the water surface has negligible effect on peak pressure. Most pile driving noise spectra have dropped to no more than 10% of their peak by a frequency of around 4 kHz. To replicate such data, sampling with a time resolution of 0.1 ms would suffice. If source and hydrophone are at a horizontal range and depths such that a few samples (say 4) of the direct arrival are taken before the surface reflection arrives then the peak pressure will not be affected by the reflection. This criterion requires a delay of 0.4 ms (which corresponds to a path difference in water of 0.6 m). In this paper, results for peak pressure will be presented only if the path difference between direct arrival and surface reflection is at least 0.6 m.

PILE VIBRATION

Equations of motion in the pile

The problem of a cylindrical shell being struck longitudinally has been modelled analytically only with a view to determining axial stress [5-7]. The similar problem of a solid slender cylindrical rod being struck by an incompressible mass has also been addressed [9, 10]. Although both of these analyses were concerned only with axial vibration, they did present concepts that are useful in analysing the generation of radial waves. In a general analysis of a rod vibrating at given frequency, a solution was obtained for the case in which torsion is absent and the axial and radial vibrations are independent of azimuth angle [9]. Using the boundary condition that the normal and shear stresses on the cylinder's lateral surface are zero, it was shown that for a slender rod the axial propagation speed is given approximately by

$$q_y = \sqrt{Y / \rho_s} \tag{1}$$

where Y and ρ_s are the Young modulus and density of the solid material. For steel, q_y is nominally 5000 m/s (whereas the separate sound and shear waves that occur in a steel block large in all three dimensions have speeds of approximately 5700 and 3100 m/s respectively).

In an analysis of an infinite cylindrical shell in-vacuo subject to an external pressure, equations of motion for each of the three types of vibration (axial, radial and azimuthal) have been presented [8]. Cylindrical axial and radial co-ordinates were used (z and r), and the respective components of displacement were denoted by u and w. It was assumed that the only external loading (p_a) acts normally to the cylindrical surface of the shell and is independent of azimuth. If torsion and bending are neglected, the equations of motion simplify to the following

$$u''(z, t) + w'(z, t)\, v/a - \ddot{u}(z, t)/q_h^2 = 0 \tag{2}$$

$$u'(z, t)\, v / a + w(z, t)/a^2 + \ddot{w}(z, t)/q_h^2 = p_a/\rho_s\, q_h^2\, h \tag{3}$$

where a is the cylinder external radius, h the wall thickness, z is distance along the cylinder axis from an arbitrary position, and t is time. Above each displacement (u or w), apostrophes and dots denote partial differentiation with respect to axial distance and time respectively. In a thin shell, there is no variation with radius. The symbol q_h is defined by

$$q_h = q_y / \sqrt{1 - v^2} \tag{4}$$

in which v is the Poisson ratio of the shell material. The bending rigidity of the shell is characterised by $h^2/12a^2$ [8]. This rigidity is neglected here, and the only term in which h appears in either of the equations of motion is the external loading term.

Initial velocity of pile face

The initial velocity of the pile face is obtained by applying the principle of momentum conservation to the infinitesimal bottom layer of the hammer and the infinitesimal top layer of the pile that are compressed during an infinitesimal time δt following impact [5]. The hammer is assumed to be a solid vertical cylinder made of the same material as the pile, and to have the same radius. The thicknesses of the infinitesimal

layers will both be $q_y\ \delta t$. Before impact, the total momentum ($v_h \delta M$) of these two layers is that of the bottom layer of the hammer

$$v_h \delta M = v_h\, \rho_s \pi a^2 q_y \delta t$$

where v_h is the hammer velocity. After impact both the bottom face of the hammer and the top face of the pile have a common velocity (v_0) and the total momentum will be

$$v_0 \delta M + v_0 \delta m = v_0\, \rho_s \pi a^2 q_y \delta t + v_0\, \rho_s A q_y \delta t$$

where $A = 2\pi a h$ is the area of the annular pile face. Equating the prior and subsequent momentums yields

$$v_0 = v_h / [1 + 2h/a] \tag{5}$$

For the [4] case, a = 0.381 m, h = 0.0254 m and v_h = 7.6 m/s; Eq. (5) produces an estimate of 6.7 m/s for v_0.

Initial conditions at impact

Since Eqs. (2) and (3) each have second order time derivatives their solutions will require two initial conditions. It is sufficient for each to specify two variables at one time for all vertical distances (depths) z. The pertinent initial conditions when $t = 0$ are that (a) the axial particle velocity is 0 at all values of z except $z = 0$ where it is v_0; (b) the radial particle velocity is zero for all z; and (c) both axial and radial displacements at $t = 0$ are zero for all z.

Boundary conditions at pile face

Since Eq. (2) also has a second order depth derivative, its solution will need two boundary conditions. It is necessary to provide two specifications of variables at any depths where events occur (the single depth $z = 0$ in the present scenario). It is also necessary that these specifications be applicable at all $t \geq 0$. One boundary condition is that since the pile is semi-infinite in length there will be an outgoing wave (for which the depth of a particular feature of an acoustic wave increases with time) but no incoming wave. If it did not include a term in w, Eq. (2) would be a wave equation in u with phase speed q_h. It will be assumed that the term in w does not cause reflections and that, as applies to the solution of any such wave equation in which z increases with time, the displacement will be a function of z-$q_h t$ as a single variable (rather than of z+$q_h t$). The second boundary condition arises from the mutual equation of motion for the hammer base and pile face (which remain in contact for a semi-infinite pile, since there is no reflection). The hammer compresses the pile face, which in return decelerates the hammer. The longitudinal stress at the pile face equals the product of Young modulus and strain. The strain ($\partial u/\partial z$) near the pile face is negative since at a fixed time $t > 0$, u decreases monotonically with z to zero at $z = q_h t$. Since the hammer will be decelerated, its equation of motion will be

$$M\ddot{u}(0,t) = AY \partial u(z,t) / \partial z \quad (z = 0) \tag{6}$$

where M is the hammer mass (axial strain in the hammer is neglected here). Since $u = u(z\text{-}q_h t)$ and thus $\frac{\partial u}{\partial z} = -\frac{1}{q_h}\frac{\partial u}{\partial t}$, Eq. (6) becomes

$$\ddot{u}(0,t) = -\Omega\, \dot{u}(0,t) \tag{7}$$

in which $\Omega = AY/Mq_h$. Solving Eq. (7) for axial velocity of the pile face, while taking account of the initial value of the axial particle velocity (v_0), yields

$$\dot{u}(0,t) = v_0 \exp(-\Omega\, t) \ , \ t \geq 0 \tag{8}$$

Integration of Eq. (8) yields

$$u(0,t) = v_0/\Omega\, [1 - \exp(-\Omega\, t)] \ , \ t \geq 0 \tag{9}$$

The pile-face axial displacement asymptotes to v_0/Ω with increasing time.

A note on Fourier Transforms

In succeeding sections, Fourier Transforms (FT) will be taken of displacements and pressures as functions of time. In the mathematical definition of the forward FT, the integrand is the product of the function of time and exp (-$i\omega t$), while in the inverse Fourier Transform (IFT) the integrand is the product of the function of frequency and exp (+$i\omega t$) ($\omega = 2\pi f$, f being frequency). In recent decades, many publications written by physicists or engineers, including textbooks referred to in this paper, have interchanged these definitions. Since the numerical component of the present work uses routines in the International Mathematics and Statistics Library (IMSL), which conforms to the mathematical definition, that definition is adopted here. This definition is consistent with the assumption that the time dependence of a single-frequency (harmonic) variable is exp (+$i\omega t$) rather than exp (-$i\omega t$). Fourier Transforms of individual variables (u, w and p) will be denoted by the corresponding capital letters (U, W and P).

Boundary condition at the pile wall

If the pile is submerged in fluid, then Eq. (2) is unaffected but in Eq. (3) p_a changes from pressure applied to a cylinder in-vacuo to pressure exerted on the cylinder by the external compressible medium as a result of the cylinder's vibration (the pile radial vibration induces strain in the external fluid). The basic equation of acoustic motion in the fluid adjacent to the wall is

$$\partial p(r,z,t)/\partial r = -\rho \ddot{w}(z,t) \tag{10}$$

the FT of which is

$$\partial P(r,z,\omega)/\partial r = \omega^2 \rho W(z,\omega) \tag{11}$$

In deriving a relation between pressure and vibration at the wall, it will be assumed that the cylinder vibration is a downward travelling wave with an (initially unknown) phase velocity G which may be complex and vary with frequency. For time dependence exp (+$i\omega t$) the appropriate dependence on depth is exp (-$i\omega z/G$), and the radial vibration FT is expressed as

$$W(z,\omega) = W(0,\omega) \exp(-i\omega z/G) \tag{12}$$

Because the wave equation is separable in cylindrical co-ordinates, it follows from Eq. (11) that the depth-dependence

of P must be the same as that of W [8], and may be expressed as

$$P(r,z,\omega) = R(r)\exp(-i\omega z/G)$$

Taking the FT of the wave equation in $p(r,z,t)$ produces the Helmholtz equation

$$\nabla^2 P + (\omega^2/c^2)\, P = 0$$

which yields the Bessel equation of order 0 for $R(r)$

$$R'' + R'/r + \xi^2 R = 0 \tag{13}$$

where

$$\xi^2 = \omega^2 / c^2 - \omega^2/G^2 \tag{14}$$

Since the Hankel function of the second kind gives the appropriate dependence on range for time dependence exp ($+i\omega t$), the solution to this equation is $H_0^{(2)}(\xi r)$. The FT of the radiated pressure at horizontal range r from the cylinder axis is therefore given by

$$P(r,z,\omega) = A(z,\omega) H_0^{(2)}(\xi r) \tag{15}$$

where $A(z,w)$ must be chosen so that the acoustic particle velocity in the fluid adjacent to the cylinder surface equals the wall radial velocity. Using Eq. (15) to obtain $\partial P / \partial r$ yields

$$\partial P(r,w) / \partial r = -A(z,w)\xi H_1^{(2)}(\xi r) \tag{16}$$

Substituting Eqs. (11) and (12) into (16) yields A in terms of W

$$A(z,\omega) = -\rho\omega^2\, W(0,\omega) \exp(-i\omega z/G) / \xi H_1^{(2)}(\xi a) \tag{17}$$

hence

$$P(r,z,\omega) = -\rho\omega^2\, W(0,\omega) \exp(-i\omega z/G)\, H_0^{(2)}(\xi r) / \xi H_1^{(2)}(\xi a) \tag{18}$$

The FT of the Specific Acoustic Impedance (Z) at the wall ($r = a$) is thus

$$Z(a,\omega) = P(a,z,\omega)/i\omega W(z,\omega) = i\omega\rho H_0^{(2)}(\xi a) / \xi H_1^{(2)}(\xi a) \tag{19}$$

As would be expected from Eq. (11), Z is independent of z.

Solving the equations of motion

Equation (2) is an equation of motion in u but includes a term in w', while Eq. (3) is an equation of motion in w that includes a term in u'. In order to allow for effects that may be frequency dependent, these two equations are solved simultaneously by taking the FT of each. Since loading pressure is opposite in sign to radiated pressure, the FT of p_a in Eq. (3) ("P_a") is replaced by $P_a = -i\omega WZ$, and the following equations in U and W are obtained

$$U'' + W' v/a + (\omega^2/q_h^2)\, U = 0 \tag{20}$$

$$vU'/a + W / a^2 - (\omega^2/q_h^2)\, W = - i\omega W Z_n/\rho_s h\; q_h^2 \tag{21}$$

in which the subscript n can have values of 1 or 2, denoting air and water respectively. The available information on $\dot{u}(z,0)$ has not been used in deriving Eqs. (20) or (21); it was instead used in deriving Eq. (9), which will be referred to later. Eq. (21) simplifies to

$$W = - v q_h^2 U' / a S_n^2(q_h) \tag{22}$$

where

$$S_n(q_h) = \sqrt{q_h^2/a^2 - \omega^2 + i\omega\, Z_n/p_s h} \quad , n = 1, 2 \tag{23}$$

The feedback to W caused by the pressure it generates in the external fluid is represented by the third term in Eq. (23) which, since it depends on ξ and hence on G, is unknown at this stage.

Axial vibration

Since Z_n does not vary with depth, differentiating Eq. (22) with respect to z and then substituting W' into Eq. (20) will yield

$$U'' + \omega^2/V_n^2(\omega)\, U = 0 \tag{24}$$

where

$$V_n(\omega) = q_h\, S_n(q_y)/S_n(q_h) \tag{25}$$

Since Eq. (24) is a standard Helmholtz equation with a depth-independent coefficient, $V_n(\omega)$ will be the phase velocity of the solution for U.

The next step is to find the appropriate solution to Eq. (24). The general solution is

$$U(z,\omega) = F(\omega) \exp(-i\omega z/V_n) + F_2(\omega) \exp(+i\omega z/V_n) \tag{26}$$

The terms in Eq. (26) correspond to waves travelling in opposite directions along the z axis, and it is necessary to determine which term corresponds to z increasing with time. Since the time dependence is exp ($+i\omega t$), the second term would result in u(z,t) depending on $t + z/V_n$, which is inappropriate, as discussed prior to Eq. (6). It follows that $F_2 = 0$.

Since q_y, q_h and Z_n and hence V_n are independent of z (within a given medium), the solution to Eq. (24) may be written as

$$U_n(z,\omega) = F(\omega) \exp(-i\omega z/V_n) \tag{27}$$

By taking the FT of Eq. (9) it can be seen that $F(\omega) = v_0/i\omega(\Omega + i\omega)$.

Radial Vibration

Differentiating Eq. (27) with respect to depth yields

$$U_n'(z,\omega) = -v_0 \exp(-i\omega z/V_n)/V_n(\Omega + i\omega) \tag{28}$$

Substituting Eq. (28) into Eq. (22) yields

$$W_n(z,\omega) = \chi \exp(-i\omega z/V_n)/S_n(q_y)\, S_n(q_h)(\Omega + i\omega) \tag{29}$$

where

$$\chi = \nu v_0 q_h / a \quad (30)$$

On comparing Eq. (29) with Eq. (12) it can be seen that $G = V$ (in the current context, the dependence on medium 'n' is not significant and is suppressed for clarity). The situation is that V is a function of $S(q_y)$ and $S(q_h)$ which in turn are functions of Z and hence of V

$$V = \varphi(V) \quad (31)$$

where φ is the function represented by Eqs. (25), (23) and (19). Equation (31) is solved by iteration; one starts with a trial solution $V^{[0]}$ and then computes successive approximations [11]

$$V^{[j+1]} = \varphi(V^{[j]}) \; j = 0, 1, 2 \quad (32)$$

The iteration is terminated at $j = J$ when the ratio $|V^{[J]} - V^{[J-1]}|/|V^{[J]}|$ is sufficiently small. For the current problem, 10^{-6} was found to be suitable as the terminating ratio, and the Fortran "huge" number ($\sim 10^{38}$) was found to be suitable for $V^{[0]}$. J was observed to be 2, 3 or 4.

Spectra of phase velocity and damping rate

For an external medium of air, the iterations $V^{[1]}$ and $V^{[J]}$ are found to be indistinguishable at any frequency. The real part of $V_1(\omega)$ for the [4] case is shown in Figure 1 over frequencies from 0 to 10 kHz. It is q_y at zero frequency, and asymptotes to q_h at high frequency. The two radial resonance frequencies of a cylindrical shell are $q_y/2\pi a$ and $q_h/2\pi a$ [9]. For the [4] case the corresponding resonance frequencies are 2089 and 2183 Hz. Real $\{V_1\}$ is small at the lower resonance, and large at the higher. Thus Real $\{V_1\}$ increases rapidly from a small to a large value as frequency increases (by 4.5%) from the lower resonance to the other.

The damping rate in decibels per metre is given by

$$D = -\omega \, Imag(1/V_1) \, 20/\ln 10 \quad (33)$$

in which the factor 20/ln10 converts nepers to decibels. The result for the damping rate in air-exposed pile (D_1) for the [4] case is shown in Figure 2, over frequencies from 0 to 10 kHz. It is small at most frequencies, but large (up to 57 dB/m) at frequencies between the two resonance frequencies.

In water, the real parts that correspond to the iterations $V^{[1]}$ and $V^{[J]}$ are found to be distinguishable in the neighbourhoods of the two frequencies where they have their minimum and maximum values. The initial and final iteration values of Real $\{V_2\}$ for the [4] case are shown in Figure 3. They vary smoothly (but not monotonically) with frequency. Each is q_y at zero frequency, falls to a minimum (around 1% lower than q_y at 1.4 kHz for the [4] case), increases to a maximum (around 3% above q_h at 2.7 kHz for the [4] case), and then asymptotes to q_h as frequency increases further.

In a water medium, the damping rates that correspond to the iterations $V^{[1]}$ and $V^{[J]}$ are found to be distinguishable in the neighbourhood of the frequency where they have their maximum values. The results for the [4] case are shown in Figure 4. Each is zero at zero frequency, and rises to a broad peak at 2.1 kHz. If there were no absorption in the pile, D_2 would asymptote to zero as frequency approaches and passes 10 kHz. The presence of absorption in steel with Q=500 [12] causes both D_1 and D_2 to asymptote to a linear increase with frequency (and reach 0.53 dB /m at 50 kHz).

One difference between a shell and solid cylinder is that, as may be seen from Figures 1 and 3, the propagation speed of high-frequency axial vibrations along a shell is higher by a ratio of q_h/q_y. For steel (ν = 0.29) the high-frequency propagation speed along a thin shell is 4.5% higher than along a solid rod, giving a nominal value of 5225 m/s. The rationale for these behaviours can be seen by considering the three terms in each of the numerator and denominator of Eq. (25), as given in Eq. (23). The constant terms, which are the only terms that differ between numerator and denominator, are respectively q_h^2/a^2 and q_y^2/a^2. At high frequencies, the functions $S_n(q_y)$ and $S_n(q_h)$ will asymptote to a common value (and V will asymptote to q_h) when either the terms in ω^1 exceed the constant terms, or the terms in ω^2 exceed the constant terms. At low frequencies, these functions will approach different values.

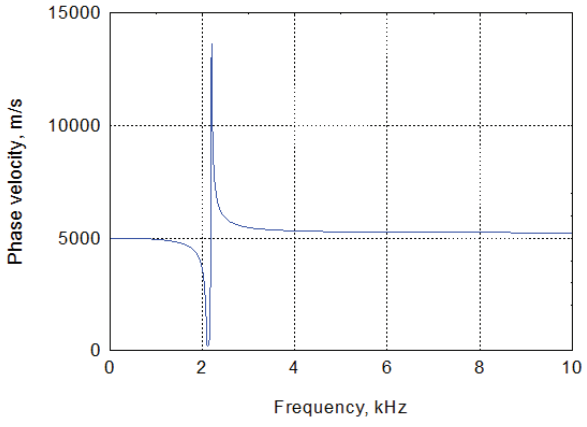

Figure 1. Real part of phase velocity in the air-exposed portion of a pile for the [4] case

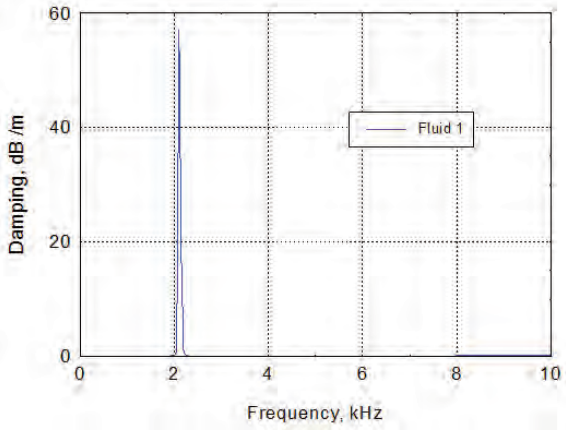

Figure 2. Damping rate in the air-exposed portion of a pile for the [4] case

Damping of shell vibration with axial distance

The cylinder material is modelled with a small loss factor, represented by making the Young modulus complex and assigning to it an imaginary part of Y/Q. Any additional damping must be attributed to the loss of energy through acoustic radiation. It follows from Eqs. (27) and (29) that, at angular frequency ω:

(a) axial and radial phase speeds are both V_n (which approaches q_y as frequency approaches zero in both air and water);

(b) axial and radial damping rates are both - Imag $\{\omega/V_n\}$ nepers per unit depth.

The next step is to compute W_2 at depth z below the water surface, according to:

$$W_2(H,z,w) = \chi \exp(-i\omega H/V_1 - i\omega z/V_2)/S_2(q_y)S_2(q_h)(\Omega + i\omega) \quad (34)$$

where H is the height of the pile face above the water surface. Attenuation of W_2 with increasing H or z is computed automatically due to the positive imaginary parts of V_1 and V_2.

To enhance clarity in distinguishing between depth along the pile and hydrophone depth, the latter will henceforth be denoted by a different symbol (ξ) in any context where they could be different in principle. In view of the assumption that the peak pressure at position (r,ξ) will arrive from that portion of the pile at the same depth (the closest), ξ and z will generally have the same value in the present derivation. For the [4] case, H = 5.4 m and the minimum and maximum values of ξ were 4.9 and 10.5 m. The magnitudes of the spectrum $|W_2(H,z,\omega)|$ at both z = 4.9 and 10.5 m are shown in Figure 5 (in decibels). Although the spectra were computed with a Nyquist frequency of 50 kHz, the maximum frequency shown is 10 kHz (the results at higher frequencies did not reveal any unexpected features). It can be seen that the high damping in the air-exposed pile between the radial resonance frequencies causes a deep minimum there, and that the spectra decay significantly with depth, especially between 1 and 4 kHz. The results for W that correspond to the iterations $V^{[1]}$ and $V^{[J]}$ are found to be indistinguishable at any frequency.

The IFTs of $W_2(H,z,\omega)$ have been calculated at both z = 4.9 and 10.5 m and the magnitudes of the resulting waveforms $|w_2(H,z,t)|$ are shown in Figure 6. The waveforms rise rapidly to peaks of around 170 and 152 μ and then decay quasi-exponentially with a time constant of 3 ms. Compared with the shallower waveform, the deeper waveform is 1 ms later, and its amplitude is 11% smaller.

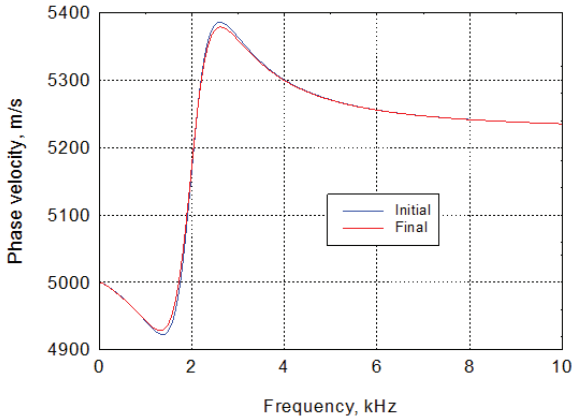

Figure 3. Real part of Phase velocity in the water-exposed portion of a pile for the [4] case: Blue (first iteration); red (final iteration).

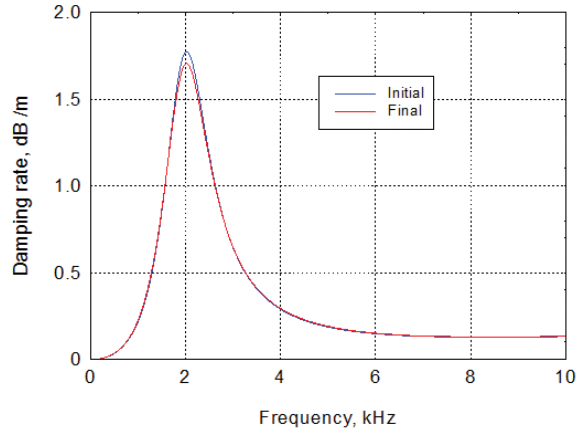

Figure 4. Damping rate in the water-exposed portion of a pile for the [4] case: Blue (first iteration); red (final iteration)

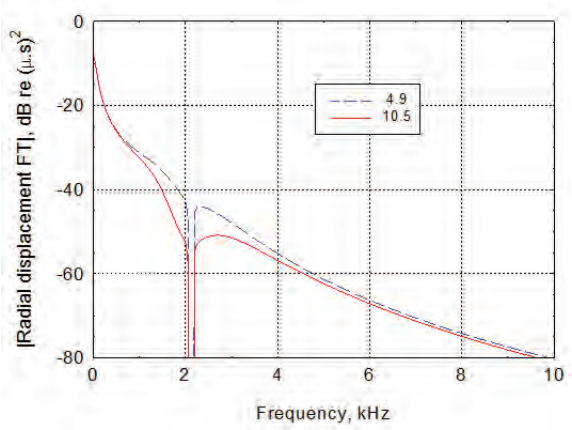

Figure 5. Magnitude of the radial displacement spectra at depths in water of 4.9 and 10.5 m for the [4] case

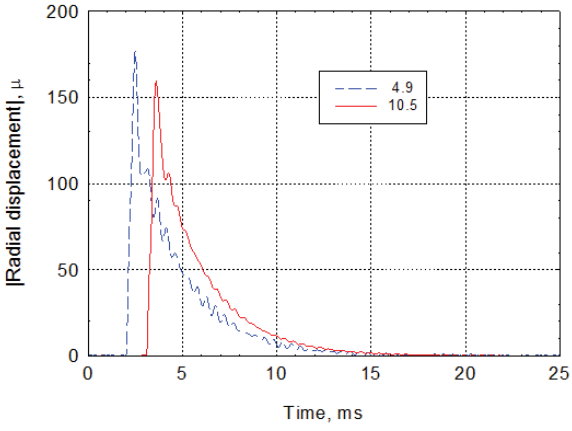

Figure 6. Magnitude of the radial displacement waveforms at depths in water of 4.9 and 10.5 m for the [4] case

UNDERWATER RADIATED SOUND PRESSURE

The sound pressure radiated into the surrounding fluid by a vertical cylinder will be computed using two models for acoustic radiation from a vibrating cylinder. The first model assumes that the cylinder vibration is independent of depth, and the second allows for it to vary with depth. Both models assume the external medium to be fluid, homogeneous and unbounded. The sound speed and density of the external medium will be denoted by c and ρ.

Depth-independent cylinder vibration

If an infinite vertical cylinder were to vibrate radially with a depth-independent amplitude, then $V(\omega)$ would be infinite, ξ would become ω/c and $P(r,z,\omega)$ would be given by a simplified version of Eq. (18)

$$P(r,z,\omega) = -\rho c\omega W(0,\omega) \exp(-i\omega z/V)\, H_0^{(2)}(\omega r/c)/\, H_1^{(2)}(\omega a/c) \quad (35)$$

If V were treated consistently as infinite, then the exponential term in Eq. (35) would be unity. Equation (35) would be independent of z and equivalent to that presented by [13] for radiation from an infinite cylinder vibrating uniformly. The exponential term will be retained here however, and Equation (35) will be referred to as the "hybrid Morse" model. For the [4] case, r = 12 m, and the magnitudes $|P(12,z,\omega)|$ computed from Eq. (35) are shown in Figure 7. $W(H,z,\omega)$ is again given by Eq. (34) for both z = 4.9 and 10.5 m, and H = 5.4 m. Since Eq. (35) will give the exact pressure spectrum only if W is independent of depth, these results are approximate; they assume that the cylinder vibrates at all depths with the value computed at z.

The IFTs of $|P(12,z,\omega)|$ have been computed for both z = 4.9 and 10.5 m, and the resulting waveforms $|p(12,z,t)|$ are shown in Figure 8. The peak pressure is 160 kPa at 4.9 m and 120 kPa at 10.5 m, a decrease of 25%.

Results have been obtained for the hybrid-Morse peak pressures for hydrophones at a range of 12 m and depths from 1 to 12 m, and are shown in Figure 9. For each of these calculations the source depth was set to the hydrophone depth. The individual data points labelled "Reinhall" are the peaks of the individual waveforms at nine hydrophone depths, as read from Figure 11 in [4]. The Reinhall results increase significantly with depth, whereas the hybrid-Morse pressures decay with depth due to the decay in $W(z,\omega)$, and are also too high. Being too high is to be expected, since this model assumes the cylinder to be infinitely long and vibrating with uniform phase.

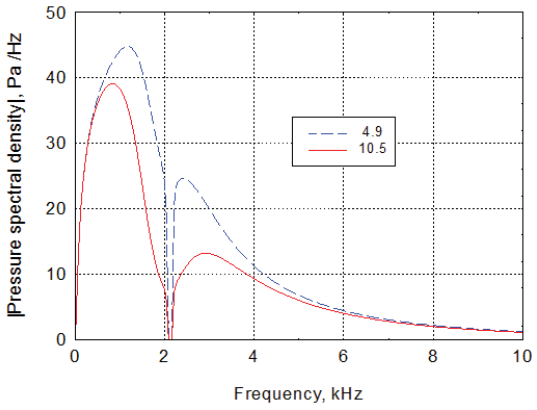

Figure 7. Magnitude of the "hybrid Morse" sound pressure spectra at depths in water of 4.9 and 10.5 m for the [4] case. Obtained by applying the Morse acoustic model to $W(z,\omega)$ as per Eq. (34)

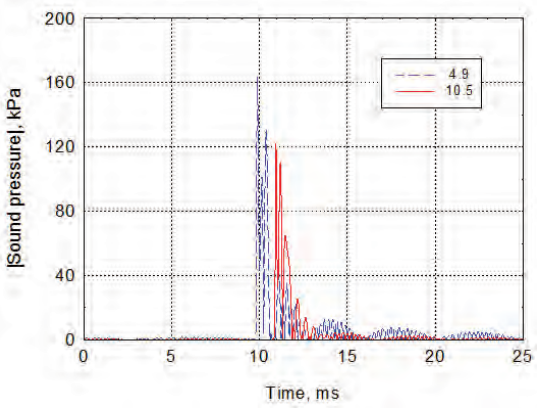

Figure 8. Magnitude of the "hybrid Morse" sound pressure waveforms at depths in water of 4.9 and 10.5 m for the [4] case. Obtained by taking the IFTs of the spectra whose magnitudes are shown in Figure 7

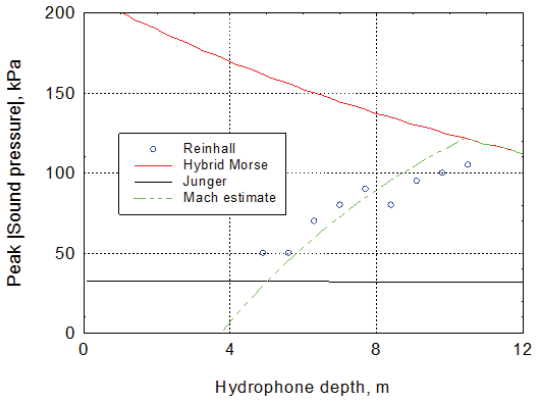

Figure 9. Peak pressure of waveforms computed for hydrophones at a range of 12 m and at depths from 0.1 to 12 m for the [4] case. 'Reinhall' refers to results read from [4], 'Hybrid Morse' refers to IFT of Eq. (35), 'Junger' refers to IFT of Eq. (38), and 'Mach Estimate' refers to Eq. (42)

Depth-dependent cylinder vibration

A method that allows for vibration to vary with distance along a cylinder has been presented by [8]. The derivation of this cylinder vibration model takes the spatial FT of the vibration's depth dependence, and uses the property that the component at each wavenumber is invariant with depth (just as a spectral component of a temporal waveform is invariant with time). The sound pressure component as a function of wavenumber is computed, and for the scenario of no azimuthal dependence, the spatial IFT presented in [8] simplifies (after converting the time dependencies) to

$$P(r,z,\omega) = \omega^2 \rho W(0,\omega) \int_{-\infty}^{\infty} H_0^{(2)}(\xi r)\, \tilde{f}(\gamma,\omega)\, \exp(i\gamma z)/2\pi\xi H_1^{(2)}(\xi a) d\gamma \quad (36)$$

where

$\xi = \sqrt{k^2 - \gamma^2}$

$k = \omega/c$

γ is axial (depth) wavenumber

$\tilde{f}(\gamma,\omega)$ is the spatial FT of the ratio $W(z,\omega)/W(0,\omega)$ as a function of z

$$\tilde{f}(\gamma,\omega) W(0,\omega) = \int_0^{\infty} W(z,\omega) \exp(-i\gamma z)\, dz \quad (37)$$

It is evident that Eq. (36) cannot cater for a radial displacement $w(z,t)$ that also varies with time due for example to motion of the sound source. A description will be required of $P(r,z,\omega)$ at various depths of the bulge below the pile face, and thus at various times. It will therefore be necessary to re-compute P at each such time.

If r is sufficiently large that the large-argument asymptotic value of the Hankel function can be used for most of the values of ξ in Eq. (36), then an approximate simple expression for the pressure spectrum can be obtained using the method of stationary phase to simplify the integral [8]. An argument of at least 2π makes the approximation reasonable, and since r = 12 for the [4] case, this assumption will be reasonable for a minimum k of 2π /12 m^{-1}, which in seawater corresponds to minimum frequency of around 125 Hz. Thus only a very small portion of the spectrum will be rendered in significant error by this approximation. According to [8], Eq. (36) will simplify to

$$P(r,\zeta,\omega) = i\rho \exp(-ikr)\omega^2 \tilde{f}(k \cos\theta,\omega) W(0,\omega)/\pi kr H_1^{(2)}(ka) \quad (38)$$

where $\theta = \arctan(r/(\zeta - z))$. Equations (36)-(38) will be referred to as the "Junger" model. If the depth of the leading edge of the bulge (z) is the same as the depth of the hydrophone (ζ) then $\theta = \pi/2$ and the first argument of the spatial FT will be zero. From Eqs. (29) and (37), the spatial FT will be given by

$$\tilde{f}(0,\omega) = \int_0^{\infty} W(z,\omega)\, dz \,/\, W(0,\omega) = V/i\omega \quad (39)$$

Taking the spatial FT of $W(z,\omega)$ renders P independent of ζ. Computed results for the spectrum $P(12,\omega)$ for the [4] case, with $\tilde{f}(0,\omega)$ given by Eq. (39), are shown in Figure 10. The peak of the spectrum is about 75% less than those of the hybrid-Morse spectra shown in Figure 7.

The corresponding pressure waveform has been obtained by taking the temporal IFT of Eq. (38), and the result is shown in Figure 11. The peak pressure is 32 kPa, which is around 80% less than the corresponding results in Figure 8. The Junger result is independent of source /hydrophone depth, since this model takes the wavenumber FT along the (infinite) length of the pile, which is independent of depth. It is ironic that a model that caters for depth-dependent cylinder vibration produces a sound pressure that is independent of depth.

The Junger peak pressure of 32 kPa for hydrophones at a range of 12 m is shown (by the horizontal line) in Figure 9. The whole Junger curve is lower than the smallest Reinhall peak pressure.

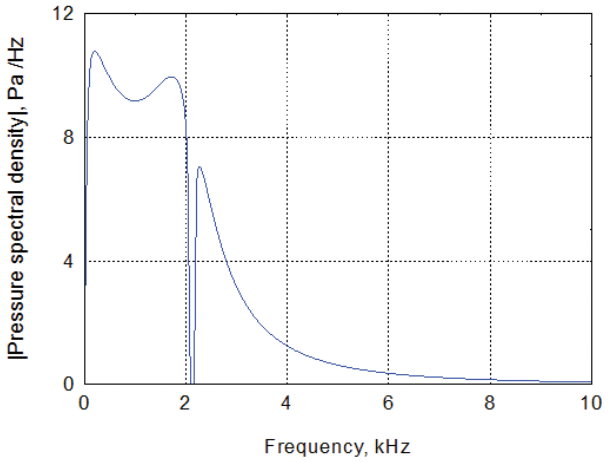

Figure 10. Magnitude of the Junger sound pressure spectrum in water for the [4] case

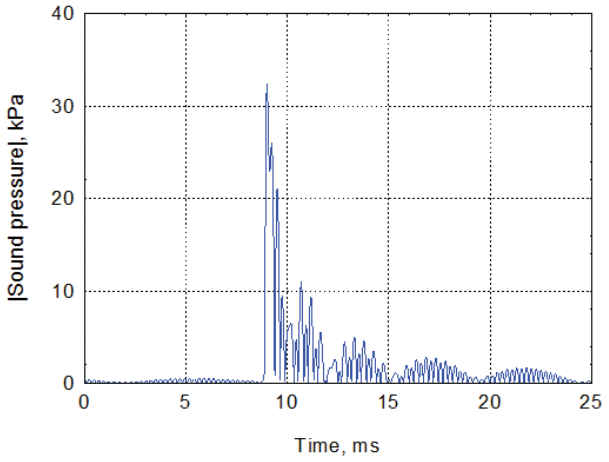

Figure 11. Magnitude of the Junger sound pressure waveform in water for the [4] case. Obtained by taking the IFT of the spectrum whose magnitude is shown in Figure 10

Estimation of Mach-wave pressures

The travel time of a pulse from a water entry at (0,0) to a hydrophone at (r,ζ) will be given by

$$t(r,\zeta) = z/q + \sqrt{(z-\zeta)^2 + r^2/c} \qquad (40)$$

where z is the depth of the bulge on the pile from which the pulse emanates. If $q > c$ then at any ζ this function has a minimum, which occurs at

$$z - \zeta = -r/\sqrt{q^2/c^2 - 1} \qquad (41)$$

In the r - z plane this corresponds to a straight line: at $r = 0$, $z = \zeta$; and $dz/dr = -1/\sqrt{q^2/c^2 - 1}$. If ϕ is the depression angle of this line relative to the horizontal r-axis, then $\tan\phi = dz/dr$ and thus $\sin\phi = c/q$. For the [4] case, $\phi = 17°$. At a given (r, ζ), the first arrival originates from position $(0, z)$ on the pile where z is given by Eq. (41). Successive pulses arrive simultaneously from points both above and below that z. (For the hybrid-Morse model for which q is effectively infinite, $\phi = 0$ and $z = \zeta$.) For source depths (z) from 0.1 to 12.5 m (the seafloor depth in the [4] case), the arrival times at range 12 m and five hydrophone depths from 4.9 to 10.5 m are shown in Figure 12. At a hydrophone depth of 7.7 m for example, the first pulse arrived at 10.3 s and originated from a depth of 4.0 m (at $r = 12$ m, Eq. (41) gives -3.7 m for $z - \zeta$).

The feature of the curves in Figure 12 that is relevant to simultaneous arrivals is the region around the minimum. For $\zeta = 7.7$ m for example, the arrival time is 10.7 s for a pulse from the surface, decreases to 10.3 at the minimum ($z = 4.0$), and then increases and attains its surface value at $z = 7.6$ m; this arrival will be referred to as the "surface-coincident" arrival. Pulses that emanated from the pile at both $z = 0$ and $z = 7.6$ m arrived simultaneously at (12,7.7), and the continuum of pulses that emanated at intervening depths all arrived within a time span of 0.4 s.

The results for source depth of both the first and surface-coincident arrivals have been computed for the [4] case and are shown as functions of hydrophone depth in Figure 13. The curves are exactly linear and quasi-linear respectively, and extrapolate to $\zeta = 3.7$ m at $z = 0$, in accordance with Eq. (41). Thus for $\zeta \leq 3.7$ m, simultaneous arrivals would not occur at a range of 12 m (although they would at a shorter range).

Since there is little variation in arrival time for source depths between zero and the surface-coincident depth (*Zsc*), it will be hypothesised that the Mach-wave pressure is due to an equivalent finite uniform (virtual) cylinder with length equal to *Zsc*. The formula postulated as an estimate of the Mach-wave pressure is

$$p\,Mach(\zeta) = p\,Morse(\zeta) \times Zsc(\zeta)/D\,, \quad Zsc \leq D \qquad (42)$$

$$p\,Mach(\zeta) = p\,Morse\,(\zeta), \qquad Zsc > D$$

where D is the seafloor depth. The results are shown in Figure 9, and are seen to be a reasonable estimate of the results reported by [4].

CONCLUSIONS

A model of the vibration of a cylindrical shell struck by a hammer has been derived with some rigour. The model includes coupling of the axial and radial vibration. It has been used to predict peak pressure of the pulse radiated into water by linking with both a "hybrid Morse" infinite cylinder and a "Junger" depth-dependent cylinder. In the first case, the predicted peak pressure is higher than reported results of an accurate Finite-Element model [4]; this is attributed to the quasi-uniform cylinder being infinite in length. The FE peak pressures increased from 50 to 100 kPa as the hydrophone depth increased from 5 to 11 m, whereas the hybrid-Morse pressure decreased from 160 to 120 kPa over the same interval. In the second case, the predicted peak pressure is constant at 32 kPa. An ad-hoc hypothesis, that the pressure is given by the product of the hybrid-Morse pressure and the ratio of hydrophone depth to seafloor depth, yields a reasonable result for the particular case that was tested.

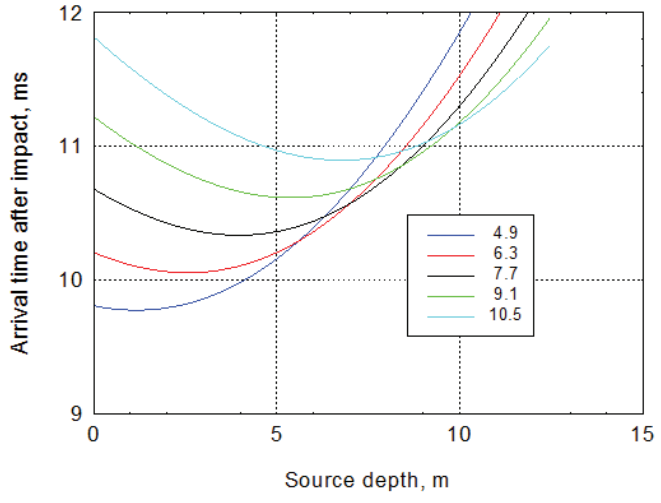

Figure 12. Arrival times at range 12 m as a function of source depth on a pile. Hydrophone depths range from 4.9 to 10.5 m in steps of 1.4 m, as indicated in the legend

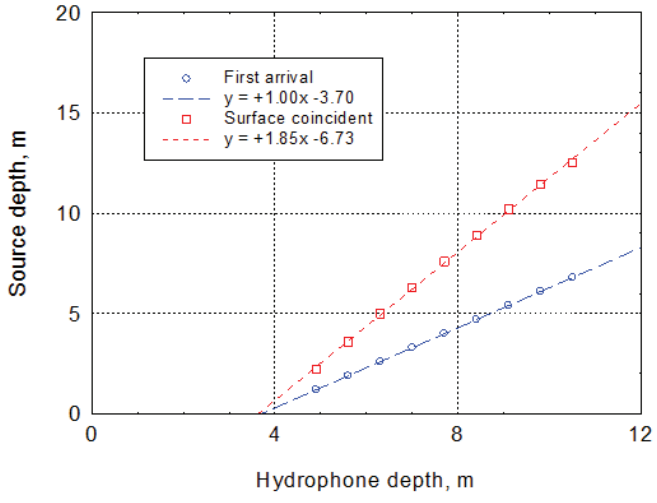

Figure 13. Source depths of both the first (Z_1) and surface-coincident arrivals (*Zsc*) as functions of hydrophone depth

ACKNOWLEDGMENT

As a result of pertinent comments by an anonymous referee, the theory is noticeably different from the initial version (although the results are only slightly different).

REFERENCES

[1] B.L. Southall, A.E. Bowles, W.T. Ellison, J.J. Finneran, R.L. Gentry, C.R. Greene Jr., D. Kastak, D.R. Ketten, J.H. Miller, P.E. Nachtigall, W.J. Richardson, J.A. Thomas, and P.L. Tyack, "Marine mammal noise exposure criteria: initial scientific recommendations", *Aquatic Mammals* **33**, 411-521 (2007)

[2] R. Matuschek and K. Betke, "Measurements of construction noise during pile driving of offshore research platforms and wind farms", *Proceedings of the NAG/DAGA 2009 International Conference on Acoustics*, Rotterdam, The Netherlands, 23-26 March 2009, pp. 262-265

[3] T.J. Carlson and M.A. Weiland, *Dynamic Pile Driving and Pile Driving Underwater Impulsive Sound*, final report, Battelle–Pacific Northwest Division, Richland, Washington, 2007

[4] P.G. Reinhall and P.H. Dahl, "Underwater Mach wave radiation from impact pile driving: Theory and observation", *Journal of the Acoustical Society of America* **130**, 1209-1216 (2011)

[5] D.V. Isaacs, "Reinforced concrete pile formulae", *The Journal of the Institution of Engineers Australia, Transactions of the Institution* **3**, 305-323 (1931)

[6] V.H. Glanville, G. Grime, E.N. Fox and W.W. Davies, *An investigation of the stresses in reinforced concrete piles during driving*, Technical Paper No. 20, Building Research, Department of Scientific and Industrial Research, London, 1938

[7] B. Hansen and H. Denver, *Wave equation analysis of a pile – an analytic model*, Technical Report No. 17, Danish Geotechnical Institute, 1984. Available at *www.geoteknisk.dk/media/5392/geo.technical.report.no.17.pdf*

[8] M.C. Junger and D. Feit, *Sound, Structures, and Their Interaction* (second edition), Acoustical Society of America, New York, 1993

[9] A.E.H. Love, *A treatise on the mathematical theory of elasticity* (fourth edition), Dover Publications, New York, 1944

[10] S.P. Timoshenko and J.N. Goodier, *Theory of elasticity* (third edition), McGraw-Hill Kogakusha Ltd, Tokyo, 1970

[11] G.A. Korn and T.M. Korn, *Mathematical Handbook for scientists and engineers* (second edition), McGraw-Hill Book Company, New York, 1968

[12] J.S. Sastry and M.L. Munjal, "Response of a multi-layered infinite cylinder to a plane wave excitation by means of transfer matrices", *Journal of Sound and Vibration* **209**, 99-121 (1998)

[13] P.M. Morse and K.U. Ingard, *Theoretical Acoustics*, McGraw-Hill Book Company, New York, 1968